Ecotoxicology and Environmental Safety 165 (2018) 423–433

Contents lists available at ScienceDirect

Ecotoxicology and Environmental Safety

journal homepage: www.elsevier.com/locate/ecoenv

Non-toxicity of nano alumina: A case on mung bean seedlings

Nisha Shabnam, Hyunook Kim*

Department of Environmental Engineering, University of Seoul, Seoul, Republic of Korea

ARTICLE INFO

Keywords:
Al_2O_3 nanoparticles
Al ions
Antioxidants
Oxidative stress
Vigna radiata

ABSTRACT

Wide use of Al_2O_3 nanoparticles (NPs) leading to their possible escape into environment and their interaction with living organisms demands immediate attention. We evaluated impact of nanoparticulate (Al_2O_3-NPs) and ionic (Al^{3+}) forms of aluminium on early seedling growth of *Vigna radiata*. While Al^{3+} inhibited growth of seedlings, Al_2O_3-NPs did not affect it negatively. Unlike enhancement in proline, malondialdehyde and H_2O_2 levels in roots and shoots induced by Al^{3+}, these stress markers remained unaltered by Al_2O_3-NPs. No signs of membrane damage were recorded in roots of seedlings raised in presence of Al_2O_3-NPs; this was witnessed from insignificant electrolyte leakage and Evans blue uptake. Activities of antioxidant enzymes, i.e., superoxide dismustase, catalase, guaiacol peroxidase in root and shoot were enhanced by Al^{3+}. However, they were unaffected by Al_2O_3-NPs. Al^{3+} enhanced levels of non-protein thiols, phenolics and ascorbate, with no alterations induced by Al_2O_3-NPs. These findings revealed that, Al_2O_3-NPs did not induce oxidative stress in seedlings. Seedlings raised in Al^{3+} showed higher uptake of Al than those grown in Al_2O_3-NPs; Al content was higher in roots. Al was not detected in shoots of seedlings grown in Al_2O_3-NPs. Lower translocation of Al in seedlings raised in Al_2O_3-NPs was due to adsorption/restriction of Al_2O_3-NPs on root surface. Al^{3+} caused ruptures on root epidermis of seedlings and inhibited root-hair formation, whereas no structural damage was caused by Al_2O_3-NPs. Our findings revealed that while ionic Al is highly toxic, nanoparticulate form of Al is non-toxic to growth of *V. radiata*.

1. Introduction

Distinct properties of materials at a nano level (< 100 nm), for examples, large surface area to volume ratio, small size and high reactivity, enable them to find applications in various industrial sectors and our daily lives (Handford et al., 2014). Owing to their wide applications, it is estimated that the global market for metal and metal oxide nanoparticles will surpass 10,000 t and 51,000 million USD by the end of 2026 in terms of production and values, respectively (https://www.futuremarketinsights.com/reports/metal-and-metal-oxide-nanoparticles-market).

Aluminium oxide or alumina (Al_2O_3) NPs are widely used in rocket propellants and explosives (Armstrong et al., 2003; De Luca et al., 2005), catalysis (Zacheis et al., 1999), electrosensors and electroanalysis (He et al., 2009), coatings (Landry et al., 2008), high performance ceramics (Tang et al., 2004), sunscreens (Lu et al., 2015), etc. Apart from their use as fillers and packing material (Sawyer et al., 2003), they find special applications in wastewater treatment technology through fabrication of smaller pore sized ultrafiltration membrane (Kim and Van der Bruggen, 2010; Savage and Diallo, 2005) for better performance index. Al_2O_3 NPs also serve as a solid phase extraction material for absorption, adsorption and preconcentration of heavy metal ions and other pollutants (Bhargavi et al., 2015; Ezoddin et al., 2010; Bhatnagar et al., 2010; Kumar et al., 2011). The extensive use of NPs raises a concern of their escape into the environment. Reports of silver NP release from fabrics during washing and the leaching of NPs from paints add to the apprehensions of NPs getting leaked into the environment (Benn and Westerhoff, 2008; Geranio et al., 2009; Kaegi et al., 2010; Zuin et al., 2014). Further, Gondikas et al. (2014) reported presence of Al_2O_3 NPs along with TiO_2 and ZnO NPs in the River Danube as a result of their release from sunscreens used by people during recreation activities.

Hence, it is essential to understand the effects that NPs can have on living organisms. Although there are numerous reports of NP toxicity

Abbreviations: CAT, catalase; DTT, dithiothreitol; EDTA, ethylene diamine tetra acetic acid; EDS, energy dispersive spectroscopy; GAE, gallic acid equivalent(s); GPX, guaiacol peroxidase; NP, nanoparticle; $NADP^+$, oxidized nicotinamide adenine dinucleotide (phosphate); NADPH, reduced nicotinamide adenine dinucleotide (phosphate); PVP, polyvinylpyrrolidone; SEM, scanning electron microscope; SOD, superoxide dismutase; TCA, trichloroacetic acid; Tris, tris-(hydroxymethyl)-aminomethane

* Corresponding author.
E-mail address: h_kim@uos.ac.kr (H. Kim).

https://doi.org/10.1016/j.ecoenv.2018.09.033
Received 15 June 2018; Received in revised form 2 September 2018; Accepted 6 September 2018
Available online 13 September 2018
0147-6513/

on living systems, there has been limited research on the impact of Al_2O_3 NPs. Few *in vitro* studies carried out with mammalian cells showed cytotoxicity and genotoxicity of Al_2O_3 NPs on reproductive cells (Di Virgilio et al., 2010) and murine macrophages cell lines (Soto et al., 2005). Al_2O_3 NPs can potentially cross cell membrane (Radziun et al., 2011), alter immune repose (Braydich-Stolle et al., 2010) and pose a high risk of cardiovascular diseases through induction of pro inflammatory response in endothelial cells (Oesterling et al., 2008). Toxicity of Al_2O_3 NPs was also reported for a few micro-organisms and planktons (Hu et al., 2009; Strigul et al., 2009; Sadiq et al., 2011) with limited literature available on the effects of Al_2O_3 NPs on plants. The reports are restricted to seed germination and root elongation wherein both non-inhibitory/positive (Doshi et al., 2008; Juhel et al., 2011; Lee et al., 2010; Lin and Xing, 2007) and negative effects have been reported (Burklew et al., 2012; Yang and Watts, 2005; Yanık and Vardar, 2015; Yanık et al., 2017).

In this paper, we have evaluated phytotoxic effects of ionic and nano aluminium on *Vigna radiata* (mung bean), a popular leguminous crop consumed by a large population. Legumes are well known for their high protein content and their role in improving the fertility of soil. The findings presented in this paper reveal the non-toxicity of nanoparticulate Al to *V. radiata* compared to its ionic counterpart.

2. Materials and methods

2.1. Materials

Seeds of *Vigna radiata* (cv-SML-668) were procured from Indian Agricultural Research Institute, New Delhi, India. $AlCl_3$ and Al_2O_3 NPs were brought from Sigma-Aldrich (Saint Louis, MO, USA). Detailed characterisation of Al_2O_3 NPs is presented in Fig. 1. As per the transmission electron micrographs, nanoparticles were irregular shaped within size range of 20–60 nm (Fig. 1A,B). Energy dispersive X-ray spectrum showed peaks specific to Al thus confirming that nanoparticles were composed of Al (Fig. 1C). In XRD spectrum, the prominent peaks noted at 2θ angles were near 35.1 (104), 37.7 (110), 43.3 (113), 52.2 (024), 57.5 (116), 66.5 (214), 68.1 (300) which corresponded to α-Al_2O_3 (corundum), confirming that nanoparticles were crystalline (Fig. 1D). The other weak peaks noted in the XRD spectrum were that of θ-Al_2O_3. Selected area electron diffraction pattern also confirmed the crystalline structure of nanoparticles (Fig. 1E).

2.2. Methods

2.2.1. Raising seedlings of Vigna radiata in presence of nanoparticulate and Ionic aluminium

For nano particulate and ionic aluminium, Al_2O_3 NPs and $AlCl_3$ were used, respectively. Equivalent concentrations (25, 50, 75, and 100 mgL^{-1}) of nano particulate and ionic Al were prepared in distilled water on the basis of aluminium content in Al_2O_3-NPs and $AlCl_3$, respectively. Al content in these solutions were confirmed through inductively coupled plasma (ICP) emission spectrometer (details given below section). Al_2O_3 NPs were sonicated for 60 min for a uniform suspension to prepare a stock solution of 1000 mgL^{-1}. Whenever used, Al_2O_3 NPs stock solution was sonicated for 30 min.

V. radiata seeds were washed with detergent, rinsed with distilled water and surface sterilized for 3–5 min using 2N% sodium hypochlorite. The seeds were then rinsed with sterile distilled water under a laminar hood. 15 seeds were inoculated in autoclaved glass bottle containing glass beads and 20 mL of test solution of ionic/

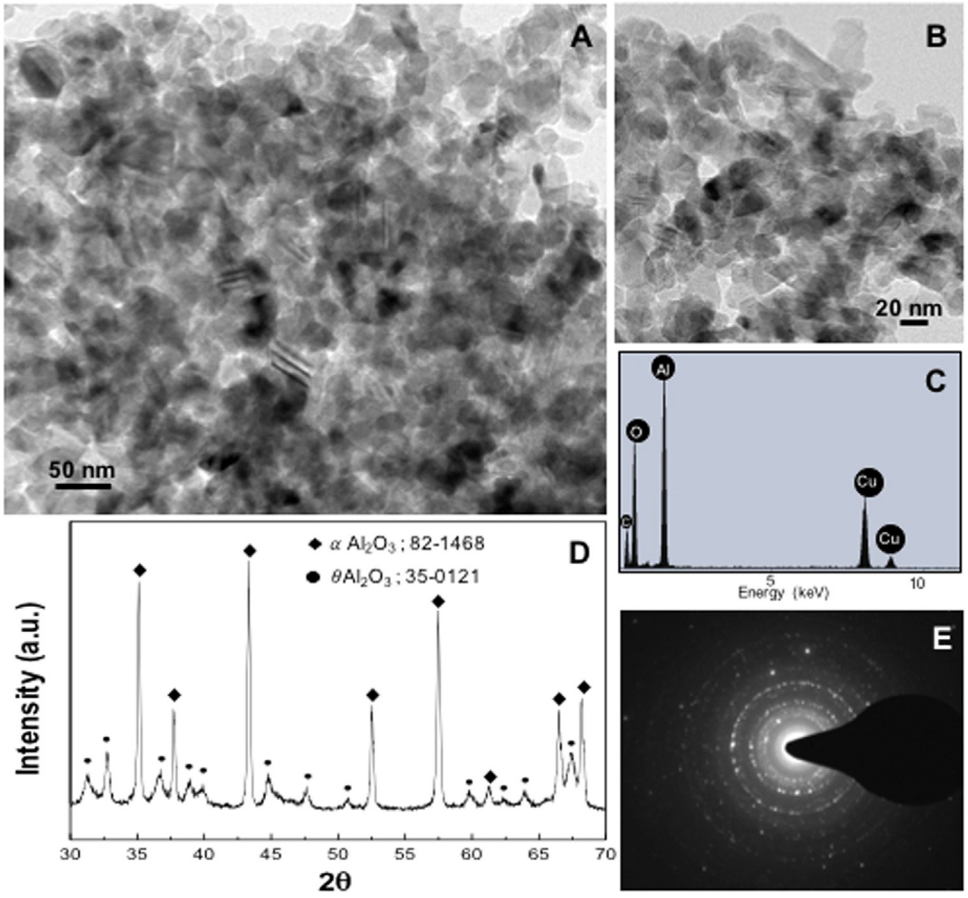

Fig. 1. Transmission electron micrographs (A, B), energy dispersive X-ray (C), X-ray diffraction (D), and selected area electron diffraction pattern (E) of Al_2O_3 nanoparticles.

nanoparticulate Al. The pH of Al_2O_3 NP solutions was/varied between 7 and 8. A separate set of glass bottles containing solutions without Al_2O_3 NPs (control) and with varying concentrations of Al_2O_3 NPs were prepared and the pH of the solutions was adjusted to that of the solutions with Al^{3+} (4.5–5) using HCl. Then, *V. radiata* seeds were inoculated into the bottles as described above. The bottles were incubated in a growth chamber at 25 ± 2 °C under a light intensity of 200 μmol photons m^{-2} s^{-1} (9/16 h light/dark cycle). No difference was observed in growth parameters in plants grown in Al_2O_3 NP treatments maintained at acidic pH compared to those grown in Al_2O_3 NP treatments at neutral-alkaline pH. Blank solutions in glass bottles without the seeds were also kept under the same condition with those with seeds. Impact of ionic and nanoparticulate Al were investigated on 8 day old seedlings.

2.2.2. Levels of proline, malondialdehyde, hydrogen peroxide

Roots and shoots of seedlings were homogenized in 5% TCA. The homogenate was centrifuged at 12,000 × *g*. For determining H_2O_2 content, samples were homogenized in chilled 5% TCA and homagenate was centrifuged at 4 °C. Levels of H_2O_2 were measured in supernatant as detailed in Shabnam and Pardha-Saradhi (2016). Proline and malondialdehyde (MDA) levels were measured in supernatant as per Shabnam et al. (2016) and Heath and Packer (1968), respectively.

2.2.3. Electrolyte Leakage

Roots and shoots were incubated in distilled water at room temperature. After 2 h, the electrical conductivity (E1) of distilled water was measured. The samples were then boiled for 30 min, cooled and electrical conductivity (E2) of solution was measured. Electrolyte leakage was measured as (EL = (E1/ E2)) and expressed as relative units based on fresh weight.

2.2.4. Staining with evans blue

The protocol of Yamamoto et al. (2001) for Evans blue staining was modified and followed. Roots were immersed in 0.025% aqueous Evans blue solution for 4 h. The roots were rinsed with distilled water until no elution of dye was observed. The roots were then homogenized in ethanol and water (v/v = 1/1). The homogenate was heated in a water bath for 30 min, then centrifuged at 12,000 × *g* for 30 min. Absorbance of the supernatant was recorded at 600 nm.

2.2.5. Enzyme activities

Roots and shoots of seedlings were homogenized in Tris-HCl buffer (50 mM, pH 7.6) consisting of 5 mM EDTA, 5% PVP, and 1 mM diothiothreitol in chilled mortal and pestle. The homogenate was centrifuged at 12,000 × *g* for 30 min at 4 °C. Supernatant was used as enzyme extract for measuring activities of various enzymes. Activities of SOD and GPX were measured as described in Shabnam and Pardha-Saradhi (2016). For SOD, reaction mixture consisting of 4 mL of 200 mM Tris-HCl buffer (pH 7.6), 200 μL L-methionine (20 mM), 200 μL EDTA (0.1 mM), 100 μL hydroxylamine (20 mM), 100 μL Triton X (0.1%), 200 μL riboflavin (0.5 mM) and 200 μL supernatant was incubated under a light intensity of 120 μmol photons $m^{-2}s^{-1}$ at room temperature. After 30 min, 2 mL of freshly prepared Greiss reagent (equal volumes of 0.1% naphthylethylenediamine dihydrochloride and 1% sulfanilamide dissolved in 5% orthophosphoric acid) was added to reaction mixture; absorbance was taken at 543 nm. Activity was calculated on basis of nitrite inhibition from a nitrite standard curve. For GPX activity, to reaction mixture consisting of 200 mM phosphate buffer (pH 6.5), 2 mM guaiacol and 20 mM H_2O_2, 50 μL supernatant was added and increase in absorbance at 470 nm was noted. Activity was calculated using extinction coefficient of 26.6 $mM^{-1}cm^{-1}$. Activity of CAT was measured following the protocol of Aebi (1984). The reaction mixture consisted of 2 mL phosphate buffer (100 mM, pH 6.5), 100 μL enzyme extract (supernatant) and100 μL of 1 mM H_2O_2. The decline in absorbance at 240 nm (due to reduction of H_2O_2) was noted at 25 ± 2 °C. Activity was calculated using extinction coefficient of 43.6 M^{-1} cm^{-1}.

2.2.6. Non-enzymatic antioxidants

Plant material was homogenized in chilled 5% TCA in a chilled mortar and pestle. The homogenate was, then, centrifuged at 12,000 × *g* for 30 min at 4 °C. Levels of ascorbate, thiols and phenolics were measured in the supernatant as described in Shabnam and Pardha-Saradhi (2016). For ascorbate determination, reaction mixture consisting of 100 μL DTT (10 mM), 100 μL N-ethylmaleimide (0.5%), 500 μL TCA (10%), 400 μL orthophosphoric acid (43%), 400 μL a-a'-bipyridyl (4%) and 200 μL $FeCl_3$ (3%) was vortexed and 200 μL supernatant was added and again vortexed. After incubation at 37 °C for 60 min, absorbance was recorded at 525 nm. For total phenolics, reaction mixture consisting of 1 mL supernatant, 1 mL Folin–Ciocalteau reagent and 2 mL Na_2CO_3 (700 mM) was incubated in dark at room temperature. After 1 h, absorbance was taken at 765 nm. For thiols, reaction mixture consisted of 200 μL supernatant, 775 μL K_2HPO_4 (500 mM) and 25 μL 5,5-dithiobis (2-nitrobenzoic acid) (10 mM in 100 mM of phosphate buffer, pH 7.0). After 15 min, absorbance was recorded at 412 nm and thiols levels were calculated using extinction coefficient of 13.6 mM^{-1} cm^{-1}.

2.2.7. Aluminium content in seedlings

Root and shoot were dried in an oven at 90 °C for 48 h. The samples were, then, digested using HNO_3 for 20 min in a BUCHI Digest Automate K-438 (New Castle, DL, USA) at 100 °C. After cooling, the samples were diluted with deionized water. To evaluate the dissolution of Al ions from Al_2O_3 NP solutions, blanks were ultra-centrifuged at 50,000 × *g* for 30 min. Supernatant was digested and finally diluted as described above. The samples were analyzed for Al content using an inductively coupled plasma (ICP) emission spectrometer (Schimazdu ICPE-9000, Kyoto, Japan). To ensure quality control, readings of the blank as well as a standard were taken after measurement of every 10 samples.

2.2.8. Scanning electron microscopic investigations

The root segments were fixed in a fixative consisting of 1% glutaraldehyde and 4% formaldehyde in 0.2 M phosphate buffer (pH 7.2) overnight (McDowell and Trump, 1976). The root segments were, then, washed with 0.2 M phosphate buffer (pH 7.2). After washed, the segments were put in distilled water and processed for freeze-drying. The dried samples were coated with Pt-Pd using HITACHI MC1000 ion sputter (Hitachi, Tokyo, Japan) and then viewed under Hitachi S-8220 field emission scanning electron microscope (Hitachi, Tokyo, Japan) with associated hardware for energy dispersive spectroscopy (EDS).

2.3. Statistical analysis

All experiments were carried out five times, each with three replicates. For growth measurements, root and shoots, ten plants were used for each set. Data are presented as mean ± standard error. The variations between the means of different concentrations of ionic and nanoparticulate Al; and between ionic and nanoparticulate Al treatment of similar concentrations were determined using Duncan multiple range test and Student *t* test, respectively.

3. Results

3.1. Growth parameters of Vigna radiata seedlings raised in presence of onic and nanoparticulate aluminium

Al_2O_3 NPs did not show any negative effect on germination as well as growth of the seedlings (Fig. 2). As shown in Fig. 2, the length, fresh weight and dry weight of roots as well as shoots of the seedlings were unaffected by Al_2O_3 NPs at concentrations as high as 100 mgL^{-1}. In contrast to non-inhibitory effects of Al_2O_3 NPs, Al^{3+} resulted in a

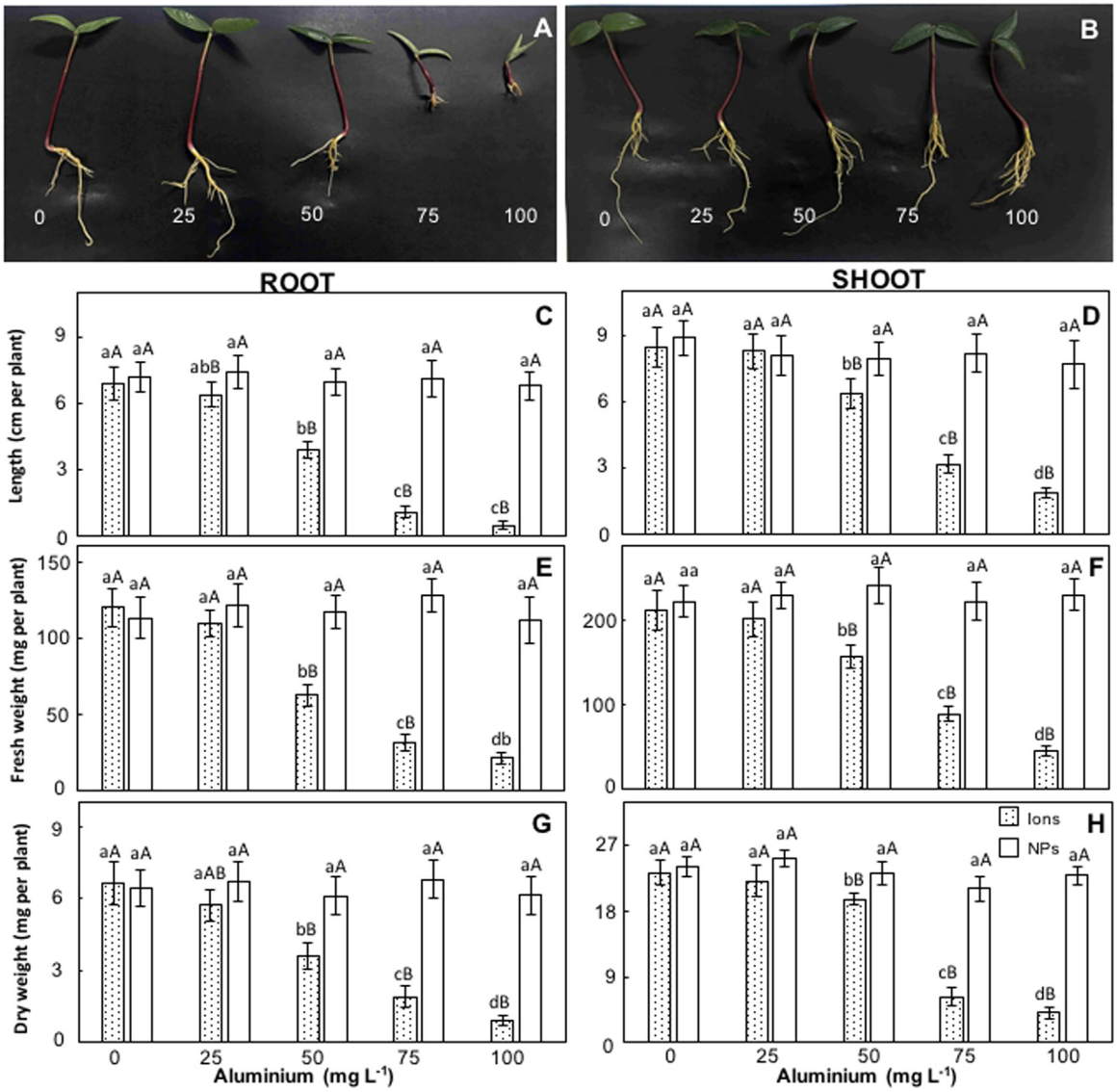

Fig. 2. Impact of ionic and nanoparticulate (NP) aluminium on growth of *V. radiata*. Seedlings of *V. radiata* raised in presence of $AlCl_3$ (A) and Al_2O_3 nanoparticles (B); length (C, D), fresh weight (E, F), and dry weight (G, H) of roots and shoots of *V. radiata*. Vertical lines on bars representi standard error. Values designated by different small letters between different concentrations of Al_2O_3 nanoparticles or $AlCl_3$ are significantly different at $P \leq 0.05$. Values designated by different capital letters between Al_2O_3 nanoparticles or $AlCl_3$ of similar concentrations are significantly different at $P \leq 0.05$.

significant reduction in all the growth parameters in roots and shoots of seedlings at concentrations ≥ 50 mgL^{-1} (Fig. 2A–H). The decrease was significantly higher in shoots than roots. At 50 mgL^{-1} Al^{3+}, while roots showed a decline of ~ 44%, shoots showed ~ 25% decline in length. Reduction in fresh and dry weight in root was ~ 48% and ~ 48% compared to 25% and ~ 15% in shoot, respectively, in presence of 50 mgL^{-1} Al^{3+}.

3.2. Oxidative stress and membrane damage in Vigna radiata Seedlings raised in presence of ionic and nanoparticulate aluminium

The levels of proline, a free amino acid and a well-known stress marker, remained unaltered in root and shoot of seedlings raised in the presence of NPs (Fig. 3A,B). In contrast, Al^{3+} caused a significant increase in proline levels in roots as well as shoots; an increase of ~ 5 folds was noted in both root and shoot of seedlings raised at 100 mgL^{-1} Al^{3+} (Fig. 3A,B), compared to that in control. Similar to proline, no variation was observed in the MDA levels in roots and shoots of seedlings raised in the presence of NPs (Fig. 3C,D). However, a significant increase was induced in MDA levels of the seedlings by Al^{3+} at concentrations ≥ 50 mgL^{-1}., in both roots and shoots (Fig. 3C,D). The increase in MDA levels, at concentrations ≥ 50 mgL^{-1} Al^{3+}, was significantly higher in roots over shoots. For e.g. at 50 mgL^{-1} Al^{3+}, while roots showed ~ 4.2 times higher MDA levels, shoots showed an increase of ~ 3.4 times, compared to respective controls.

While Al_2O_3 NPs did not alter levels of H_2O_2, a significant increase was noted in the levels of H_2O_2 in roots and shoots of seedlings raised in the presence of Al^{3+} at concentrations > 25 mgL^{-1}, the increase being higher in shoots than in roots (Fig. 3E,F). For e.g. 100 mgL^{-1} Al^{3+} induced an increase of ~ 1.7 times in roots in H_2O_2 levels, the same was ~ 2.5 times in shoots. A significant increase was noted in electrolyte leakage in roots and shoots of seedlings at concentrations ≥ 50 mgL^{-1} Al^{3+}, whereas no alterations were recorded in seedlings raised in presence of NPs (Fig. 3G,H). Irrespective of the concentrations of Al^{3+} and Al_2O_3 NPs in which the seedlings were raised, the uptake of Evans blue (a membrane impermeable dye and an indicator for cell death) (Yamamoto et al., 2001) by roots of seedlings grown in the presence of Al^{3+} was significantly higher than those grown in the presence of Al_2O_3 NPs; and the uptake of Evans blue by roots of seedlings grown in the presence of Al^{3+} increased in a dose-dependent manner (Fig. 4).

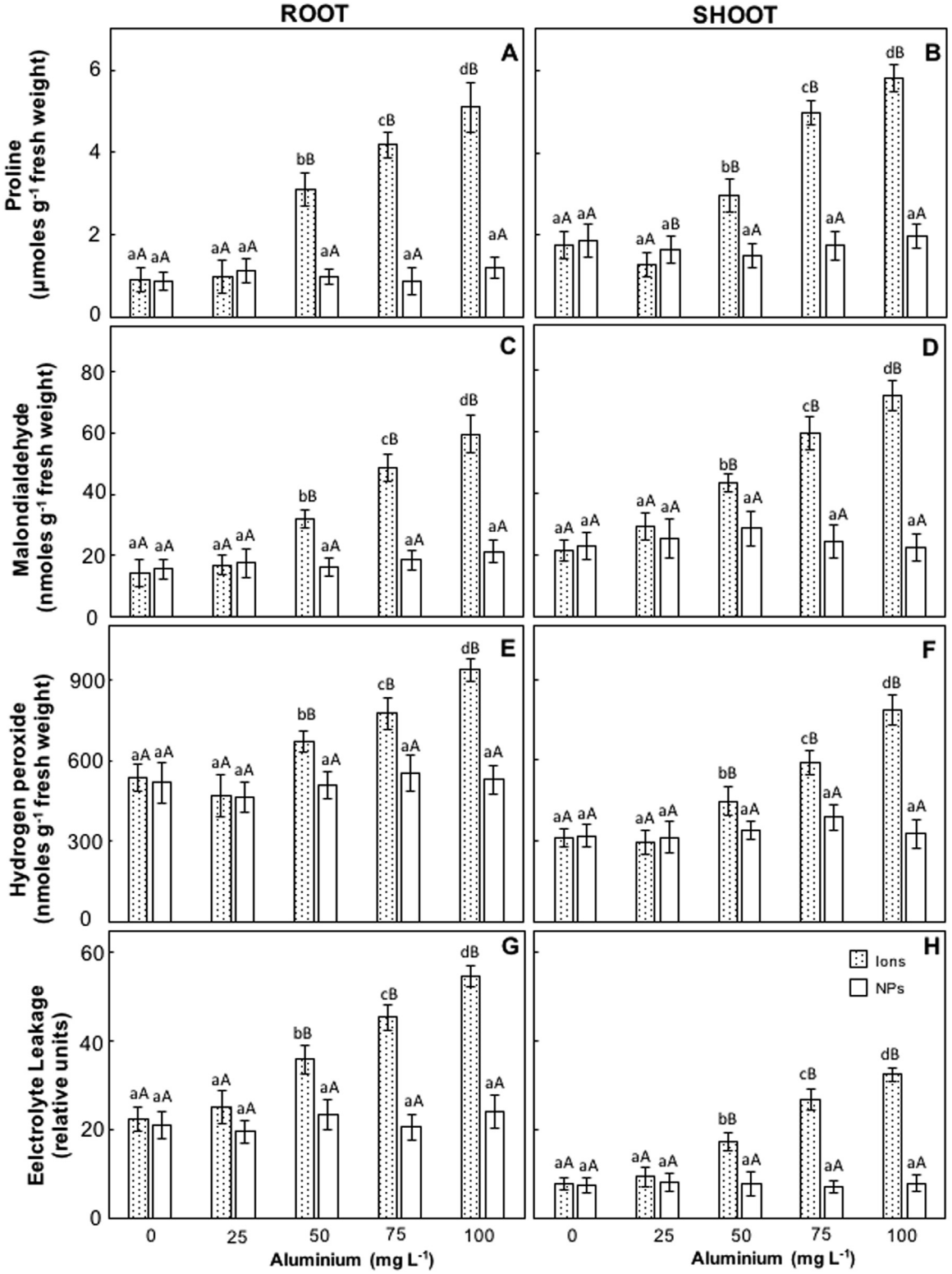

Fig. 3. Impact of ionic and nanoparticulate (NP) Al on levels of proline (A, B), malondialdehyde (MDA) (C, D), H_2O_2 (E, F) and electrolyte leakage (G, H) in roots and shoots of seedlings of *V. radiata*. Vertical lines on data bars represent standard errors. Values designated by different small letters between different concentrations of Al_2O_3 nanoparticles or $AlCl_3$ are significantly different at $P \leq 0.05$ Values designated by different capital letters between Al_2O_3 nanoparticles or $AlCl_3$ of similar concentrations are significantly different at $P \leq 0.05$.

3.3. Antioxidant status of Vigna radiata seedlings raised in presence of ionic and nanoparticulate aluminium

During the present study, Al^{3+} enhanced the activity of SOD in the seedlings at concentrations > 25 mgL^{-1}, in both root and shoot, whereas no alterations were recorded in the seedlings raised in the presence of Al_2O_3 NPs (Fig. 5A,B). Similar to H_2O_2 levels, the increase in SOD activity was significantly higher in shoots than in roots. No

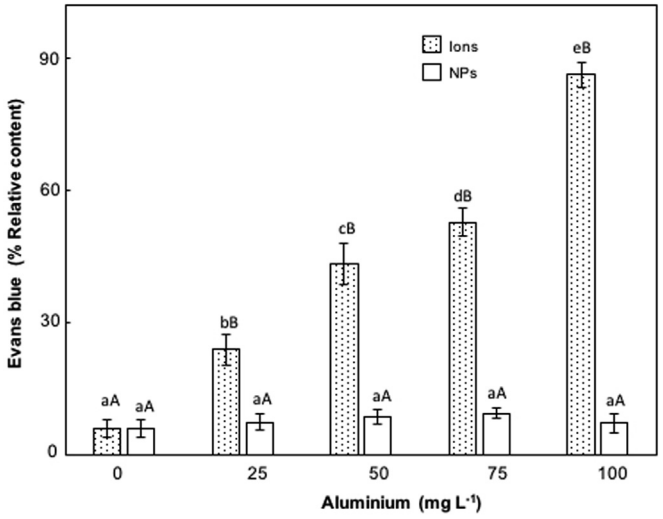

Fig. 4. Uptake of Evans blue by roots of *V. radiata* seedlings raised in presence of ionic and nanoparticulate (NP) aluminium. Vertical lines on data bars represent standard errors. Values designated by different small letters between different concentrations of Al_2O_3 nanoparticles or $AlCl_3$ are significantly different at $P \leq 0.05$. Values designated by different capital letters between Al_2O_3 nanoparticles or $AlCl_3$ of similar concentrations are significantly different at $P \leq 0.05$.

alterations were recorded in activities of CAT and GPX in root and shoot of seedlings in presence of Al_2O_3 NPs. However, Al^{3+} induced an increase in the activities of these enzymes in both roots and shoots of seedlings raised at concentrations ≥ 50 mgL^{-1} (Fig. 5C–F). At any given concentration, GPX activity was significantly higher in roots than in shoots. Also, the increase in GPX activity in both roots and shoots was higher than that observed in case of CAT. The highest increase noted in CAT activity was ~ 1.3 and ~ 1.7 folds in roots and shoots, whereas the same for GPX activity was ~ 3.1 and ~ 2.5, respectively.

Levels of phenolics and thiols, in roots and shoots of seedlings of *V. radiata* were significantly enhanced by Al^{3+} at concentrations ≥ 50 mgL^{-1} (Fig. 6A–D). However, while levels of ascorbate showed a significant increase in shoots of seedlings raised at concentrations ≥ 50 mgL^{-1}, no alterations were recorded in roots (Fig. 6E–F). Levels of all the three antioxidants were unaffected by Al_2O_3 NPs in both roots and shoots of seedlings (Fig. 6A–F).

3.4. Al content and root surface structure of Vigna radiata seedlings raised in presence of ionic and nanoparticulate aluminium

Based on distinct response of seedlings to Al_2O_3 NPs and Al^{3+}, Al content was determined in seedlings. Levels of Al were higher in seedlings raised in the presence of Al^{3+}, compared to those grown in the presence of Al_2O_3 NPs; Al content in roots was significantly higher than that recorded in shoots (Fig. 6G,H). Al content in shoots of seedlings raised at 50 mgL^{-1} Al^{3+} was ~ 70 times higher than in roots. Also, levels of Al in roots of seedlings in presence of 50 mgL^{-1} Al^{3+} was ~ 60 folds higher than those raised in presence of NPs. Negligible amount of Al was detected in shoots of seedlings grown in the presence of Al_2O_3 NPs.

Al^{3+} caused transverse ruptures on root surface (Fig. 7E). These ruptures were not observed on root surface of seedlings grown in the presence of Al_2O_3 NPs (Fig. 7I) as well as the control seedlings (Fig. 7A). In case of seedlings grown in the presence of Al_2O_3 NPs, distinct NPs/nanocomplexes were noted on the root surface. These NPs/nanocomplexes were composed of Al and oxygen, as revealed through EDS investigations (Fig. 7K, L). However, Al was not detected on root surface of the seedlings grown in presence of Al^{3+} (Fig. 7H). Roots of control seedlings showed root hairs (Fig. 7B), which were absent in roots of seedlings grown in presence of Al^{3+} (Fig. 7F). In contrast, roots of seedlings grown in presence Al_2O_3 NPs showed root hairs similar to those of the control (Fig. 7J).

4. Discussion

4.1. Nanoparticulate form of aluminium is less/nontoxic to growth of Vigna radiata seedlings than ionic aluminium

Nanoparticulate Al did not induce any alteration in growth of seedlings. These results are similar to those reported by Lee et al. (2010), Lin and Xing (2007) and Doshi et al. (2008) for various plant species, wherein no negative effect of Al_2O_3 NPs was observed. Recently, Jin et al. (2017) reported promotor effects of Al_2O_3 NPs on root growth of *A. thaliana*. However, negative effects were reported in several plants on exposure to NPs at very high concentration ranging from 1000 to 10,000 mgL^{-1}. In the study by Burklew et al. (2012), toxic symptoms were recorded in tobbacco plants during germination stage at 1000 mgL^{-1}. In wheat, inhibiting response was recorded at 5000 mgL^{-1} after exposure of young seedlings to nanoparticles (Yang and Watts, 2005). In case of *Zea mays* (corn), *Cucumis sativus*, *Glycine max*, *Brassica oleracea*, and *Daucus carota*, a marked decline in root growth was observed at 2000 mgL^{-1} (Yanık, and Vardar, 2015). These concentrations of Al_2O_3 NPs which induced a negative response in plants are much higher than what have been used during this study. In contrast to the non-inhibitory effects of NPs, the ionic form induced a drastic reduction in overall growth of seedlings. Aluminium is well known for its toxicity to plants wherein roots are the most easily effected part (Hammond et al., 1995; Tamás et al., 2004, 2006). Especially, Al is toxic to plants in acidic soils, due to dissolution of Al ions from the naturally occurring harmless aluminium oxides and alumino-silicates (Panda et al., 2009; Tamás et al., 2004). Al ions cause inhibition of growth in root by blocking the cell division thus resulting in stunted and brittle roots (Panda et al., 2009). Al ion-induced injury to the roots results in poor uptake of ions and water, further affecting the overall growth of plants (Panda et al., 2009; Tamás et al., 2004). Various other factors like cell wall disjunction, loss of plasma membrane integrity, alteration of cytoskeleton structure, and imbalance in Ca homeostasis, have also been considered responsible for Al toxicity (Tamás et al., 2004).

4.2. Nanoparticulate aluminium does not induce oxidative stress in Vigna radiata seedlings

Seedlings raised in presence of Al did not show any alteration in proline levels, whereas those raised in presence of ionic Al showed enhanced production of proline. Increase in proline content is a well-known mechanism for protecting plants from ROS; it plays an important role in maintaining NAD(P)H/$NAD(P)^+$ ratio and protecting enzymes (Shabnam et al., 2014, 2016). Levels of malondialdehyde (byproduct of lipid-peroxidation of membranes) were also enhanced by Al^{3+} as reported earlier (Basu et al., 2001; Hegedüs et al., 2001; Meriga et al., 2004; Yamamoto et al., 2001). Enhanced MDA levels in Al^{3+} exposed seedlings suggest that Al^{3+} promoted peroxidation of lipid membranes in seedlings; lipid peroxidation being higher in roots over shoots. Al^{3+} at concentrations > 25 mgL^{-1}, promoted formation/production of H_2O_2 in roots and shoots of seedlings, while no alterations were recorded in response to Al_2O_3 NPs. Enhanced levels of H_2O_2 were also noted in roots of Arabidopsis and barley in response to t Al^{3+} (Jin et al., 2017; Tamás et al., 2004). Al^{3+} induced increase in levels of H_2O_2 could be a result of either enhanced production through various enzymatic reactions catalyzed by superoxide dismutase (SOD), NAD(P)H oxidase, etc. (Gill and Tuteja, 2010; Shabnam and Pardha-Saradhi, 2016), or due to its decreased breakdown/scavenging by enzymes like catalase and peroxidases. ROS induced peroxidation of lipids results in increased membrane permeability thus promoting leakage of electrolytes (Bajji et al., 2002). Al^{3+} promoted electrolyte leakage in roots and shoots of

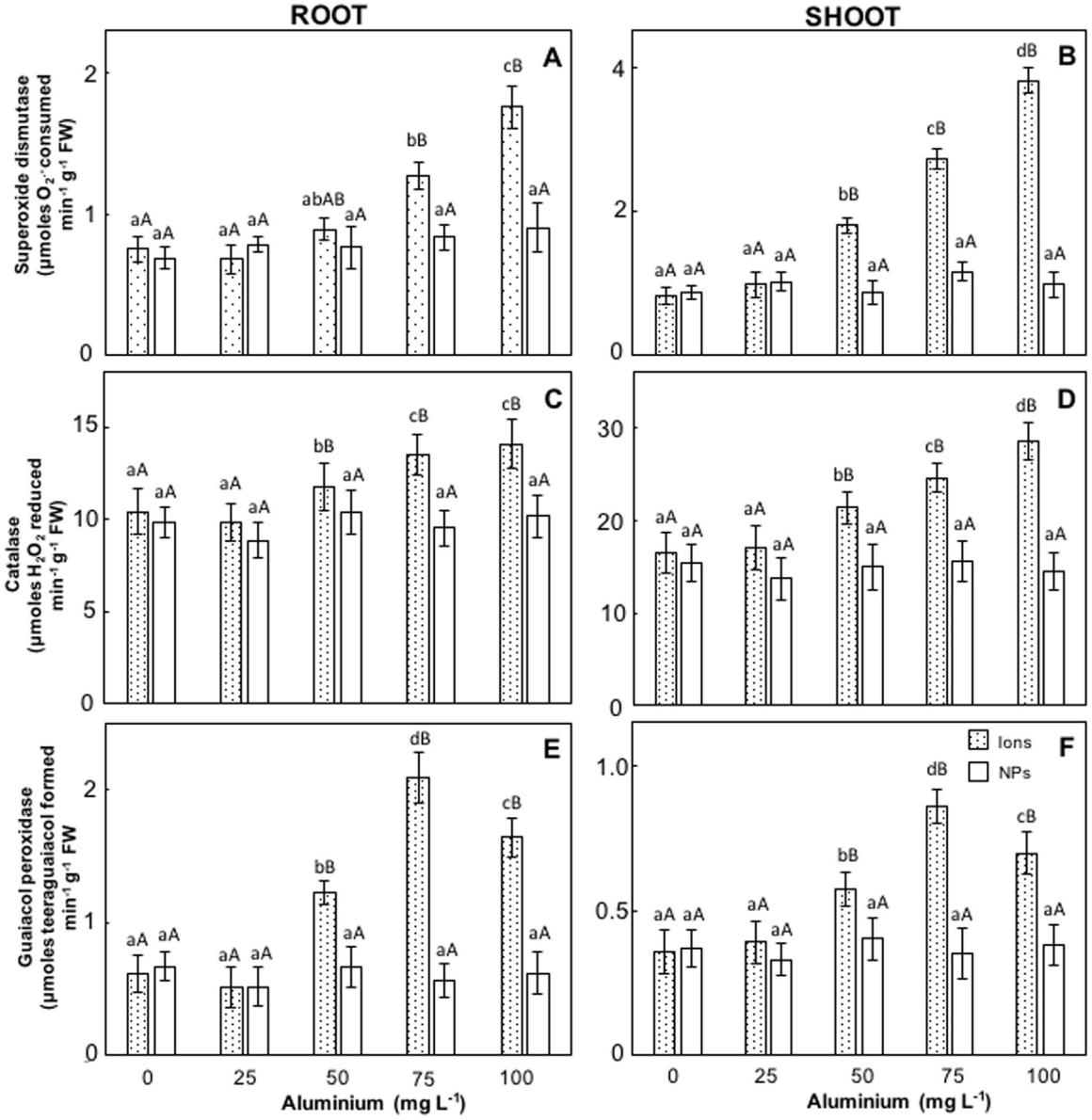

Fig. 5. Impact of ionic and nanoparticulate Al on antioxidant enzyme activities in *V. radiata*. Activities of SOD (A, B), catalase (C, D), and guaiacol peroxidase (E, F), in roots and shoots of *V. radiata* seedlings. Vertical lines on data bars represent standard errors. Values designated by different small letters between different concentrations of Al_2O_3 nanoparticles or $AlCl_3$ are significantly different at $P \leq 0.05$ Values designated by different capital letters between Al_2O_3 nanoparticles or $AlCl_3$ of similar concentrations are significantly different at $P \leq 0.05$.

the seedlings suggesting that enhanced ROS production by Al^{3+} cause lipid peroxidation of membranes resulting in a loss of membrane integrity and stability. Al^{3+} induced loss of membrane integrity in roots was also corroborated by increased uptake of Evans blue by roots of the seedlings, as reported in roots of pea and barley on exposure to Al ions (Yamamoto et al., 2001; Tamás et al., 2006). Insignificant uptake of Evans blue by roots of seedlings grown in presence of Al_2O_3 NPs suggests that nanoparticulate form of Al did not impair integrity of plasma membrane and promote cell death. Evans blue uptake along with electrolyte leakage and MDA data reveal that nanoparticulate form of Al, unlike the ionic form, do not cause any damage to membrane(s) through either disintegration of plasma membrane or peroxidation of lipids.

Superoxide anion radical, $O_2^{\cdot-}$, formed from O_2 via single-electron transfer process is highly reactive and form highly toxic hydroxyl radical ($OH^{\cdot}$) through Fenton's reaction and Haber Weiss reaction (Fukai and Ushio-Fukai, 2011; Gill and Tuteja, 2010; Shabnam and Pardha-Saradhi, 2016).). Superoxide dismutase (SOD) serves as the major defense against $O_2^{\cdot-}$ by converting it to H_2O_2 (Fukai and Ushio-Fukai, 2011; Shabnam and Pardha-Saradhi, 2016). Unaltered SOD activity of seedlings in presence of Al_2O_3 NPs revealed that nanoparticulate Al did not disturb the cellular homeostasis in seedlings which is also corroborated by unaltered levels of H_2O_2. Enhanced SOD activity was also noted in various plants in response to Al and other metal ions (Basu et al., 2001; Gupta et al., 2009; Jin et al., 2017). Enhanced activity of SOD caused by Al^{3+} suggests (i) efficient dismutation of $O_2^{\cdot-}$ to H_2O_2 which is also corroborated by increased levels of H_2O_2; and (ii) higher potential of ionic Al in inducing oxidative stress by promoting generation of $O_2^{\cdot-}$ compared to its nanoparticulate counterpart·H_2O_2 can easily diffuse across the membranes and and negatively affects various cellular functions through protein damage and lipid peroxidation (Gill and Tuteja, 2010; Shabnam and Pardha-Saradhi, 2016). H_2O_2 is scavenged by catalase and peroxidase; catalase reduces H_2O_2 into water and oxygen, while guaiacol peroxidase utilize H_2O_2 it to oxidize a variety of aromatic substrates like phenols (Gill and Tuteja, 2010; Shabnam and Pardha-Saradhi, 2016). Activities of both CAT and GPX in

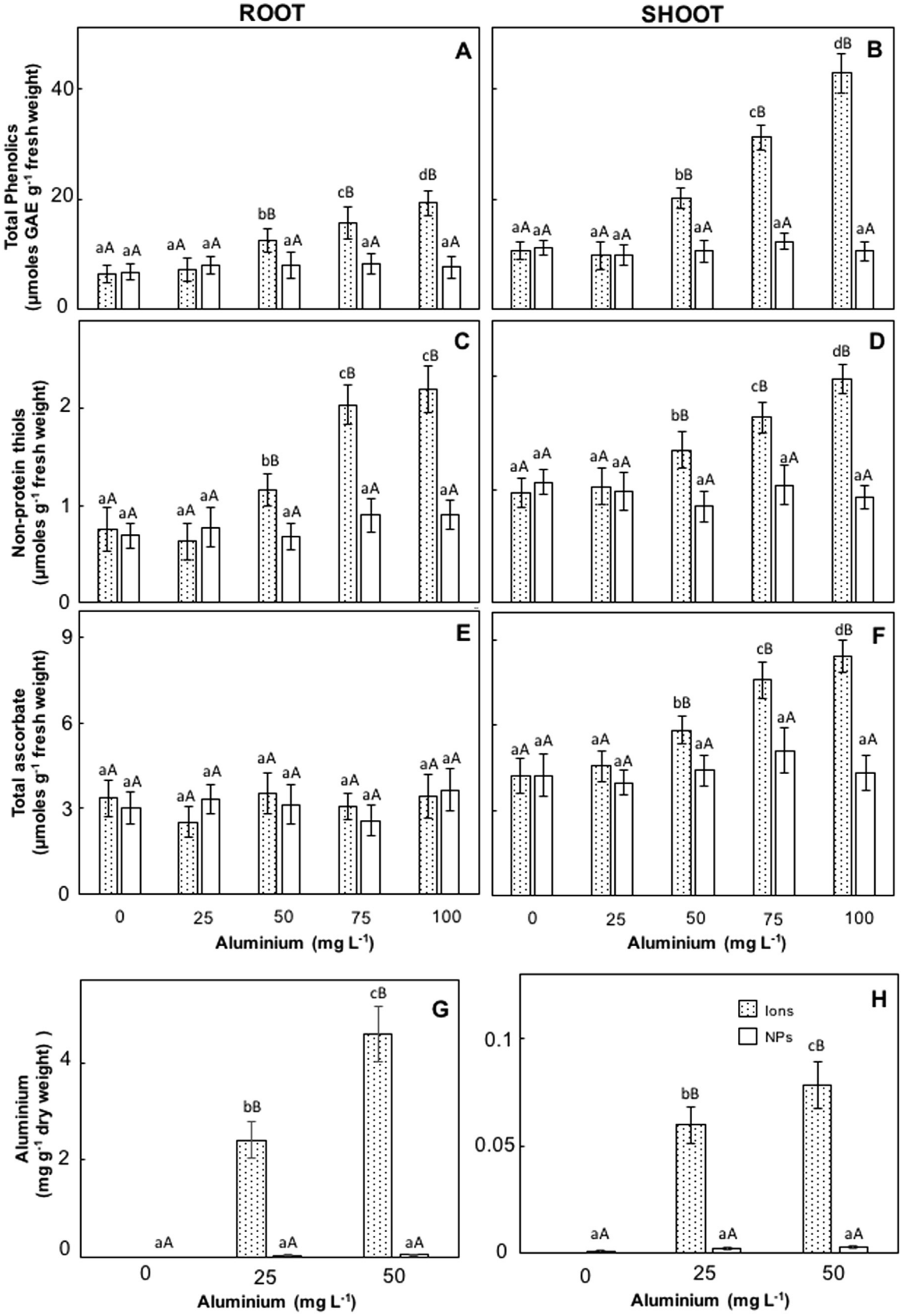

Fig. 6. Impact of ionic and nanoparticulate Al on antioxidants in *V. radiata.* Total phenolics (A, B), non protein thiols (C, D) total ascorbate (E, F) and Al content (G, H) in roots and shoots of *V. radiata* seedlings. Vertical lines on data bars represent standard errors. Values designated by different small letters between different concentrations of Al_2O_3 nanoparticles or $AlCl_3$ are significantly different at $P \leq 0.05$. Values designated by different capital letters between Al_2O_3 nanoparticles or $AlCl_3$ of similar concentrations are significantly different at $P \leq 0.05$.

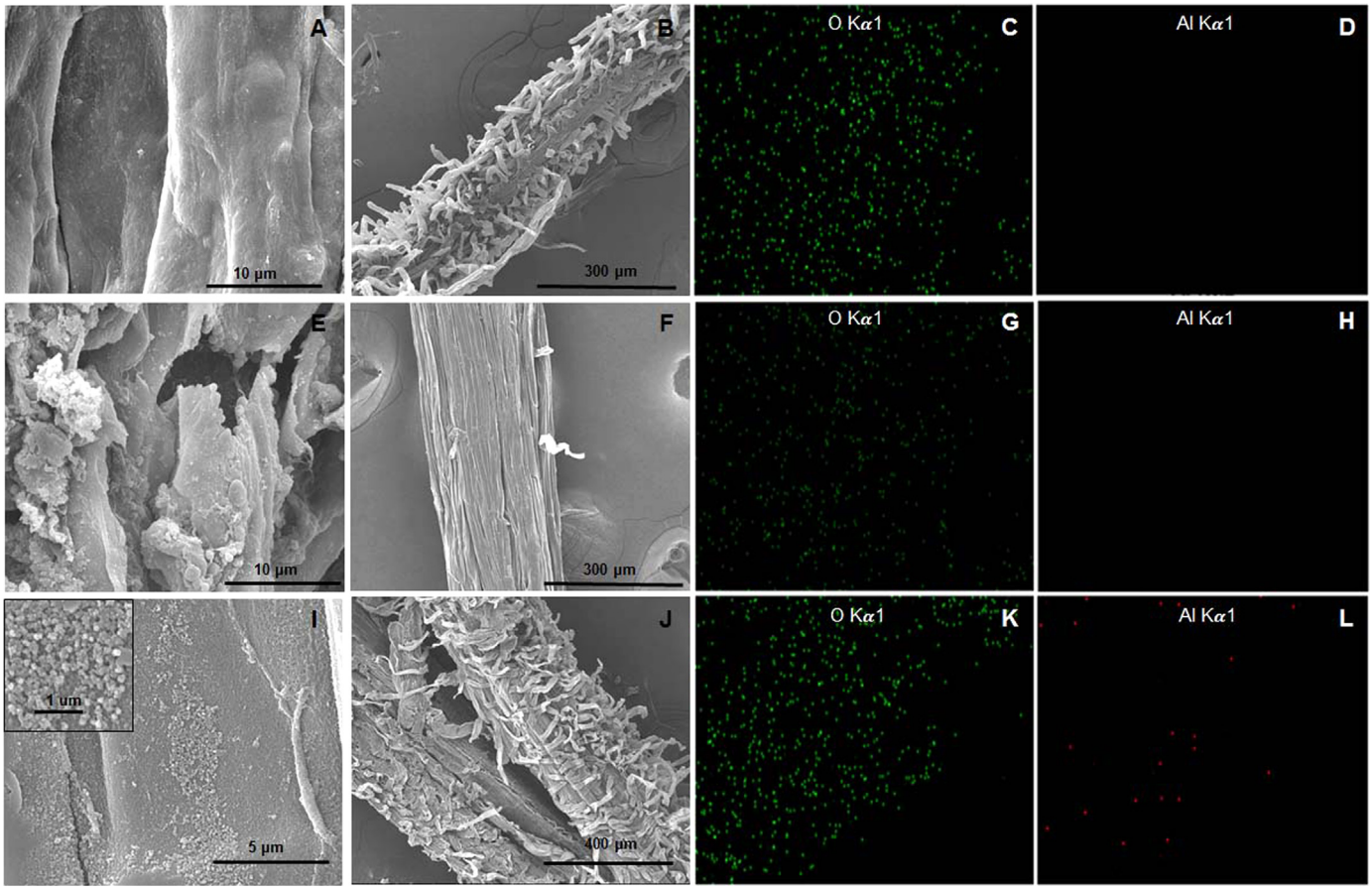

Fig. 7. Scanning electron micrographs (A, B, E, F, I, J) and EDS maps (C, D, G, H, K, L) of root surface of *V. radiata* seedlings raised in absence of (A–D) and presence of ionic (E–H) and nanoparticulate aluminium (I-L). Inset in (I) show magnified image of Al_2O_3 NPs on surface of roots of seedlings grown in presence of Al_2O_3 NPs.

seedlings were enhanced by Al^{3+} but, unaffected Al_2O_3 NPs. The coordinated increase in the activities of CAT and GPX is similar to that reported in mustard and barley under Zn and Cd stress (Hegedüs et al., 2001). Recently, Jin et al. (2017) also reported an increase in activities of CAT and GPX, which was attributed to an increased transcription of the genes involved with these enzymes. Al^{3+}-induced increase in activities of these enzymes could be due to enhanced expression of the concerned genes at transcriptional and translational levels or post-translation regulation of the protein.

A strong non-enzymatic antioxidant system comprising of molecules capable of scavenging ROS and chelating metal ions, helps plants to fight against oxidative stress (Gill and Tuteja, 2010; Shabnam et al., 2017). Among the antioxidant molecules, phenolics, ascorbate, and thiol compounds (which include glutathione, cysteine, methionine, and phytochelatins) are the predominant ones (Gill and Tuteja, 2010; Shabnam et al., 2017). Al^{3+} enhanced production of these antioxidant cellular entities while no alterations were induced by Al_2O_3 NPs. This could be due to upregulation and/or enhanced transcription of the genes involved in biosynthesis of these antioxidants as reported by Jin et al. (2017)·H_2O_2 serves as an electron donor for phenolics to participate in formation of lignin (catalyzed by peroxidase) which is responsible for thickening of cell wall (Matsumoto and Motoda, 2012; Shabnam et al., 2017). An increase in levels of H_2O_2 and phenolics with concomitant increase in GPX activity can enhance the production of lignin. Increased levels of thiols have been attributed to enhanced synthesis of phytochelatins for chelation of metal ions like Pb, Cd (Gupta et al., 2009). Till date, however, there is no report available on the role of phytochelatins in chelation of Al ions. The role of phenolics in scavenging of ROS is well established (Shabnam et al., 2014). Hence, enhanced levels of ascorbate, thiols, and phenolics in seedlings grown in presence of Al^{3+} could be a mechanism to counter the toxic ROS produced under Al stress. Overall, unaltered levels of MDA and H_2O_2, in coordination with unialtered activities of SOD, CAT, and GPX, and antioxidant levels in seedlings raised in the presence of Al_2O_3 NPs clearly revealed that nanoparticulate Al did not induce oxidative stress in the seedlings.

4.3. Nanoparticulate aluminium is restricted to the root surface of Vigna radiata seedlings without causing any damage to root surface

Higher levels of Al in seedlings raised in ionic Al than the nanoparticulate form revealed that Al^{3+} could be easily translocated in to seedlings than the latter; a major proportion of Al being translocated to roots. However, no detectable levels of Al were detected in shoots of seedlings grown inpresence of Al_2O_3 NPs. These findings suggest that nanoparticulate Al has a lower potential to enter roots of *V. raidata* seedling compared to the ionic form. The uptake of Al and other metals during early growth is well documented (Hammond et al., 1995; Peralta al, 2001). The restricted transport of Al_2O_3 NPs into the seedlings could be one of the reasons behind the non-inhibitory effects of nanoparticulate Al on growth and antioxidant status of seedlings, compared to Al^{3+}.

Nanoparticulate Al did not induce any negative effect on root structure, whereas ionic caused transverse ruptures on the epidermis of root surface of seedlings. Such ruptures on root surface have been reported in roots of other plants (e.g., cowpea) on exposure to Al and other metal ions (Kopittke et al., 2008; Horst et al., 2010; Matsumoto and Motoda, 2012; Yamamoto et al., 2001). These ruptures were presumed to be a result of breakdown and separation of rhizodermis and outer cortical cells from the layer of inner cortical cells (Kopittke et al.,

2008) or differential cell expansion due to inhibited root elongation (Yamamoto et al., 2001). It is believed that Al ion-caused ruptures on the root surface are related with increased rigidity of the cell wall (Kopittke et al., 2008; Matsumoto and Motoda, 2012). Ionic Al also inhibited formation of root hairs as reported by Jin et al. (2017) and Panda et al. (2009). These results reveal that unlike the ionic form, nanoparticulate form of Al does not disrupt root surface of seedlings of *V. radiata* and affect formation of root hairs. It is also clear from the results that Al_2O_3 NPs are retained on the root surface, thus restricting their entry into root cells. This is also evident from the ICP data which revealed a lower amount of Al in the roots of seedlings grown in the presence of nano particulate Al than those grown in ionic Al. Al_2O_3 NPs adsorbed on the root surface could be responsible for majority of the Al content in the roots of seedlings grown in presence of Al^{3+}.

5. Conclusions

The findings presented in this paper reveal that the nanoparticulate form of aluminium does not have any negative impact on the early seedling growth of *V. radiata*. Unlike the ionic form, nano particulate Al did not (i) induce oxidative stress in the seedlings and (ii) cause any damage to the membrane either through ROS-induced peroxidation of fatty acids in the lipid bilayer or through its disintegration. This non-toxicity of the nanoparticulate Al is attributed to a significantly lower translocation of Al into *V. radiata* seedlings since Al_2O_3 NPs were adsorbed and/or restricted to their root surface without causing any structural damage to the roots. In summary, our findings revealed the non-toxicity of Al_2O_3 NPs on early seedling growth of *V. radiata*. The results would further add to the existing information on interaction between aluminium nanoparticles and plants and thus call for a better evaluation of its potential risk in the environment.

Acknowledgments

We thank Prof. Sun-Hyung Kim, Department of Horticulture, University of Seoul, for the use of freeze drying and ultracentrifuge facilities. This research was performed as a part of the project, Pilot scale application of algae monitoring and nutrients removal and utilization technology (과제번호) is financially supported by Korea Ministry of Environment (MOE; Project No-2015001790002), which is greatly appreciated.

References

Aebi, H., 1984. Catalase in vitro. Methods Enzymol. 105, 121–126.
Armstrong, R.W., Baschung, B., Booth, D.W., Samirant, M., 2003. Enhanced propellant combustion with nanoparticles. Nano Lett. 3, 253–255.
Bajji, M., Kinet, J.-M., Lutts, S., 2002. The use of the electrolyte leakage method for assessing cell membrane stability as a water stress tolerance test in durum wheat. Plant Growth Reg. 36, 61–70.
Basu, U., Good, A.G., Taylor, G.J., 2001. Transgenic *Brassica napus* plants overexpressing aluminium-induced mitochondrial manganese superoxide dismutase cDNA are resistant to aluminium. Plant Cell Environ. 24, 1269–1278.
Benn, T.M., Westerhoff, P., 2008. Nanoparticle silver released into water from commercially available sock fabrics. Environ. Sci. Technol. 42, 4133–4139.
Bhargavi, R.J., Maheshwari, U., Gupta, S., 2015. Synthesis and use of alumina nanoparticles as an adsorbent for the removal of Zn(II) and CBG dye from wastewater. Int. J. Ind. Chem. 6, 31–41.
Bhatnagar, A., Kumar, E., Sillanpää, M., 2010. Nitrate removal from water by nano-alumina: characterization and sorption studies. Chem. Eng. J. 163, 317–323.
Braydich-Stolle, L.K., Speshock, J.L., Castle, A., Smith, M., Murdock, R.C., Hussain, S.M., 2010. Nanosized aluminum altered immune function. ACS Nano 4, 3661–3670.
Burklew, C.E., Ashlock, J., Winfrey, W.B., Zhang, B., 2012. Effects of aluminum oxide nanoparticles on the growth, development, and microRNA expression of tobacco (*Nicotiana Tabacum*). PLoS One 7, e34783.
De Luca, L.T., Galfetti, L., Severini, F., Meda, L., Marra, G., Vorozhtsov, A.B., Sedoi, V.S., Babuk, V.A., 2005. Burning of nano-aluminized composite rocket propellants. Combust. Explos. Shock. Waves 4, 680–692.
Di Virgilio, A.L., Reigosa, M., Arnal, P.M., de Mele, M.F.L., 2010. Comparative study of the cytotoxic and genotoxic effects of titanium oxide and aluminium oxide nanoparticles in Chinese hamster ovary (CHO-K1) cells. J. Hazard. Mater. 177, 711–718.
Doshi, R., Braida, W., Christodoulatos, C., Wazne, M., O'Connor, G., 2008. Nano-aluminum: transport through sand columns and environmental effects on plants and soil communities. Environ. Res. 106, 296–303.
Ezoddin, M., Shemirani, F., Abdi, Kh, Saghezchi, M.K., Jamali, M.R., 2010. Application of modified nano-alumina as a solid phase extraction sorbent for the preconcentration of Cd and Pb in water and herbal samples prior to flame atomic absorption spectrometry determination. J. Hazard. Mater. 178, 900–905.
Fukai, T., Ushio-Fukai, M., 2011. Superoxide Dismutases: role in redox signaling, vascular function, and diseases. Antioxid. Redox Signal. 15, 1583–1606.
Future market insights, 2018. 〈https://www.futuremarketinsights.com/reports/metal-and-metal-oxide-nanoparticles-market〉/01/10.
Geranio, L., Heuberger, M., Nowack, B., 2009. The behavior of silver Nanotextiles during washing. Environ. Sci. Technol. 43, 8113–8118.
Gill, S.S., Tuteja, N., 2010. Reactive oxygen species and antioxidant machinery in abiotic stress tolerance in crop plants. Plant Physiol. Biochem. 48, 909–930.
Gondikas, A.P., von der Kammer, F., Reed, R.B., Wagner, S., Ranville, J.F., Hofmann, T., 2014. Release of TiO_2 nanoparticles from sunscreens into surface waters: a one-year survey at the old Danube recreational lake. Environ. Sci. Technol. 48, 5415–5422.
Gupta, D.K., Nicoloso, F.T., Schetinger, M.R.C., Rossato, L.V., Pereira, L.B., Castro, G.Y., Srivastava, S., Tripathi, R.D., 2009. Antioxidant defense mechanism in hydroponically grown *Zea mays* seedlings under moderate lead stress. J. Hazard. Mater. 172, 479–484.
Hammond, K.E., Evans, D.E., Hodson, M.J., 1995. Aluminium/silicon interactions in barley (*Hordeum vulgare* L.) seedlings. Plant Soil 173, 89–95.
Handford, C.E., Dean, M., Henchion, M., Spence, M., Elliott, C.T., Campbell, K., 2014. Implications of nanotechnology for the agri-food industry: opportunities, benefits and risks. Trends Food Sci. Technol. 40 (2), 226–241.
He, Q., Zheng, D., Hu, S., 2009. Development and application of a nano-alumina based nitric oxide sensor. Microchim. Acta 164, 459–464.
Heath, R.L., Packer, L., 1968. Photoperoxidation in isolated chloroplast. I. Kinetics and stoichiometry of fatty acid peroxidation. Arch. Biochem. Biophys. 125, 189–198.
Hegedüs, A., Erdei, S., Horváth, G., 2001. Comparative studies of H_2O_2 detoxifying enzymes in green and greening barley seedlings under cadmium stress. Plant Sci. 160, 1085–1093.
Horst, W.J., Wang, Y., Eticha, D., 2010. The role of the root apoplast in aluminium-induced inhibition of root elongation and in aluminium resistance of plants: a review. Ann. Bot. 106, 185–197.
Hu, X., Cook, S., Wang, P., Hwang, H.-M., 2009. In vitro evaluation of cytotoxicity of engineered metal oxide nanoparticles. Sci. Total Environ. 407, I3070–I3072.
Jin, Y., Fan, X., Li, X., Zhang, Z., Sun, L., Fu, Z., Lavoie, M., Pan, X., Qian, H., 2017. Distinct physiological and molecular responses in *Arabidopsis thaliana* exposed to aluminum oxide nanoparticles and ionic aluminum. Environ. Poll. 228, 517–527.
Juhel, G., Batisse, E., Hugues, Q., Daly, D., van Pelt, F.N.A.M., O'Halloran, J., Jansen, M.A.K., 2011. Alumina nanoparticles enhance growth of Lemna minor. Aquat. Toxicol. 328–336.
Kaegi, R., Sinnet, B., Zuleeg, S., Hagendorfer, H., Mueller, E., Vonbank, R., Boller, M., Burkhardt, M., 2010. Release of silver nanoparticles from outdoor facades. Environ. Poll. 158, 2900–2905.
Kim, J., Van der Bruggen, B., 2010. The use of nanoparticles in polymeric and ceramic membrane structures: review of manufacturing procedures and performance improvement for water treatment. Environ. Poll. 158, 2335–2349.
Kopittke, P.M., Blamey, F.P.C., Menzies, N.W., 2008. Toxicities of soluble Al, Cu, and La include ruptures to rhizodermal and root cortical cells of cowpea. Plant Soil 303, 217–227.
Kumar, E., Bhatnagar, A., Kumar, U., Sillanpää, M., 2011. Defluoridation from aqueous solutions by nano-alumina: characterization and sorption studies. J. Hazard. Mater. 186, 1042–1049.
Landry, V., Riedl, B., Blanchet, P., 2008. Alumina and zirconia acrylate nanocomposites coatings for wood flooring: photocalorimetric characterization. Prog. Org. Coat. 61, 76–82.
Lee, C.W., Mahendra, Y.S., Zodrow, Y.K., Li, Y.D., Tsai, Y.Y.-C., Braam, J., Alvarez, P.J.J., 2010. Developmental phytotoxicity of metal oxide nanoparticles to *Arabidopsis Thaliana*. Environ. Toxicol. Chem. 29, 669–675.
Lin, D., Xing, B., 2007. Phytotoxicity of nanoparticles: inhibition of seed germination and root growth. Environ. Poll. 150, 243–250.
Lu, P.-J., Huang, S.-C., Chen, Y.-P., Chiueh, L.-C., Shih, D.Y.-C., 2015. Analysis of titanium dioxide and zinc oxide nanoparticles in cosmetics. J. Food Drug Anal. 23, 587–594.
Matsumoto, Motoda, H., 2012. Aluminum toxicity recovery processes in root apices. Possible association with oxidative stress. Plant Sci. 185–186, 1–8.
McDowell, E.E.M., Trump, B.F., 1976. Histological fixatives suitable for diagnostic light and electron microscopy. Arch. Pathol. Lab. Med. 100, 405–414.
Meriga, B., Reddy, B.K., Rao, K.R., Reddy, L.A., Kavi Kishor, P.B., 2004. Aluminium-induced production of oxygen radicals, lipid peroxidation and DNA damage in seedlings of rice (*Oryza sativa*). J. Plant Physiol. 161, 63–68.
Oesterling, E., Chopra, N., Gavalas, V., Arzuaga, X., Lim, E.J., Sultana, R., Butterfield, D.A., Bachas, L., Hennig, B., 2008. Alumina nanoparticles induce expression of endothelial cell adhesion molecules. Toxicol. Lett. 178, 160–166.
Panda, S.K., Baluska, F., Matsumoto, H., 2009. Aluminum stress signaling in plants. Plant Signal. Behav. 4, 592–597.
Peralta, J.R., Gardea-Torresday, J.L., Tiemann, K.J., Gomez, E., Arteaga, S., Rascon, E., Parsoms, J.G., 2001. Uptake and effects of five heavy metals on seed germination and plant growth in Alfalfa (*Medicago sativa* L.). Bull. Environ. Contam. Toxicol. 66, 727–734.
Radziun, E., Wilczyńska, J.D., Książek, I., Nowak, K., Anuszewska, E.L., Kunicki, A., Olszyna, A., Ząbkowski, T., 2011. Assessment of the cytotoxicity of aluminium oxide nanoparticles on selected mammalian cells. Toxicol. Vitr. 25, 1694–1700.
Sadiq, I.M., Pakrashi, S., Chandrasekaran, N., Mukherjee, A., 2011. Studies on toxicity of

aluminum oxide (Al_2O_3) nanoparticles to microalgae species: *Scenedesmus* sp. and *Chlorella* sp. J. Nanopart. Res. 13, 3287–3899.
Savage, N., Diallo, M.S., 2005. Nanomaterials and water purification: opportunities and challenges. J. Nanopart. Res. 7, 331–342.
Sawyer, W.G., Freudenberg, K.D., Bhimaraj, P., Schadler, L.S., 2003. A study on the friction and wear behavior of PTFE filled with alumina nanoparticles. Wear 254, 573–580.
Shabnam, N., Pardha-Saradhi, P., Sharmila, P., 2014. Phenolics impart Au^{3+}-stress tolerance to cowpea by generating nanoparticles. PLoS One 9, e85242.
Shabnam, N., Pardha-Saradhi, P., 2016. Floating and submerged leaves of *Potamogeton nodosus* exhibit distinct variation in antioxidant system as an ecophysiological adaptive strategy. Funct. Plant Biol. 43, 346–355.
Shabnam, N., Sharmila, P., Govindjee, Kim, H., Pardha-Saradhi, P., 2017. Differential response of floating and submerged leaves of long leaf pondweed, *Potamogeton nodosus,* to silver ions. Front. Plant Sci. 8, 1052.
Shabnam, N., Tripathi, I., Sharmila, P., Pardha-Saradhi, P., 2016. A rapid, ideal and ecofriendlier protocol for quantifying proline. Protoplasma 253, 1577–1582 .
Soto, K.F., Carrasco, A., Powell, T.G., Garza, K.M., Murr, L.E., 2005. Comparative *in vitro* cytotoxicity assessment of some manufactured nanoparticulate materials characterized by transmission electron microscopy. J. Nanopart. Res. 7, 145–169.
Strigul, N., Vaccari, L., Galdun, C., Wazne, M., Liu, X., Christodoulatos, C., Jasinkiewicz, K., 2009. Acute toxicity of boron, titanium dioxide, and aluminum nanoparticles to *Daphnia magna* and *Vibrio fischeri*. Desalination 248, 771–782.
Tamás, L., Šimonovičová, M., Huttová, J., Mistrík, I., 2004. Aluminium stimulated hydrogen peroxide production of germinating barley seeds. Environ. Exp. Bot. 51, 281–288.
Tamás, L., Huttová, J., Mistrík, I., Šimonovic˘ová, M., Široká, B., 2006. Aluminium-induced drought and oxidative stress in barley roots. J. Plant Physiol. 163, 781–784.
Tang, F., Fudouzi, H., Uchikoshi, T., Sakka, Y., 2004. Preparation of porous materials with controlled pore size and porosity. J. Eur. Ceram. Soc. 24, 341–344.
Yamamoto, Y., Kobayashi, Y., Matsumoto, H., 2001. Lipid peroxidation is an early symptom triggered by aluminium, but not the primary cause of elongation inhibition in pea roots. Plant Physiol. 125, 199–208.
Yang, L., Watts, D.J., 2005. Particle surface characteristics may play an important role in phytotoxicity of alumina nanoparticles. Toxicol. Lett. 158, 122–132.
Yanık, F., Aytürk, O., Vardar, F., 2017. Programmed cell death evidence in wheat (*Triticum aestivum* L.) roots induced by aluminum oxide (Al_2O_3) nanoparticles. Caryologia 70, 112–119.
Yanık, F., Vardar, F., 2015. Toxic effects of aluminum oxide (Al_2O_3) nanoparticles on root growth and development in *Triticum aestivum*. Water Air Soil Pollut. 226, 296.
Zacheis, G.A., Gray, K.A., Kamat, P.V., 1999. Radiation-induced catalysis on oxide surfaces: degradation of hexachlorobenzene on γ-irradiated alumina nanoparticles. J. Phys. Chem. B 103, 2142–2150.
Zuin, S., Massari, A., Ferrari, A., Golanski, L., 2014. Formulation effects on the release of silica dioxide nanoparticles from paint debris to water. Sci. Total Environ. 476–477 (298-30).